RF-MBE GROWN III-NITRIDES HETEROSTRUCTURES FOR HYDROGEN GAS SENSING APPLICATIONS

by

CHIN CHE WOEI

Thesis submitted in fulfilment of the requirements for the degree of Doctor of Philosophy

March 2017

ACKNOWLEDGEMENT

Undertaking this PhD has been a truly life changing experience for me and it would not have been possible to complete without the guidance and support that I received from many people.

First and foremost, I would like to thank my supervisor, Prof. Dr. Zainuriah Hassan for her valuable support and advice. It has been a wonderful experience to work under her supervision. She has demonstrated a great deal of encouragement and patience as I have grown personally and professionally. This PhD cannot be achieved without her constant feedback and guidance. Special thanks are given to my co-supervisor Dr. Yam Fong Kwong. His active guidance, support, motivation and cooperation have always kept me going ahead.

I would like to express my very great appreciation to my lab mates for their encouragement and support during the course of my research work. Finally, I would like to thank my family for their unconditional support. My parents have both encouraged and challenged me since my earliest memory, and fostered my interest in science. My wife has been a constant source of support throughout my doctoral studies, enduring the difficult times and celebrating the victories with me. Without the strength and love of my family, I would not have succeeded in my graduate studies.

TABLE OF CONTENTS

ACKNOWLEDGEMENT	ii
TABLE OF CONTENTS	iii
LIST OF TABLES	vi
LIST OF FIGURES	viii
LIST OF SYMBOLS	xii
LIST OF MAJOR ABBREVIATIONS	xiv
ABSTRAK	xvi
ABSTRACT	xviii

CHAPTER 1 : INTRODUCTION **1**

1.1	Introduction of III-nitrides	1
1.2	Introduction to hydrogen	2
1.3	Need of hydrogen sensor	3
1.4	Hydrogen sensor parameters	4
1.5	III-nitrides based hydrogen sensor	5
1.6	Motivations	7
1.7	Objectives	8
1.8	Originality of the research works	8
1.9	Organization of the thesis	9

CHAPTER 2 : LITERATURE REVIEW **11**

2.1	Introduction	11
2.2	Hydrogen technology	11
2.3	Hydrogen gas sensor technology	13
2.4	III-Nitrides based gas sensor	17
	2.4.1 AlGaN based gas sensor	19
	2.4.2 InGaN based gas sensor	21
2.5	III-Nitrides nanostructures based gas sensor	23
	2.5.1 Quantum Dots	24

2.5.2 InGaN quantum dots based gas sensor 27

CHAPTER 3: GROWTH AND CHARACTERIZATION TECHNIQUES **29**

3.1 Introduction 29

3.2 Molecular beam epitaxy 29

3.2.1 Residual gas analyzer (RGA) 32

3.2.2 Reflection high energy electron diffraction (RHEED) 33

3.3 Field emission scanning electron microscopy (FESEM) 35

3.4 Atomic force microscopy (AFM) 37

3.5 High resolution X-r ay diffraction (HRXRD) 40

3.6 Photoluminescence (PL) 42

3.7 Radio frequency (RF) magnetron sputtering system 43

CHAPTER 4: EXPERIMENTAL **45**

4.1 Introduction 45

4.2 Substrate preparation 45

4.3 Growth of AlN buffer layer 49

4.4 Growth of GaN thin films 51

4.5 Growth of AlGaN thin films 52

4.6 Growth of InGaN thin films 53

4.7 Growth of InGaN quantum dots (QDs) 53

4.8 Characterization of III-nitrides thin films 54

4.9 Fabrication of hydrogen gas sensor 54

4.10 Characterization of gas sensor 55

4.11 Summary 57

CHAPTER 5: RESULTS AND DISCUSSION **59**

5.1 Introduction 59

5.2 Analysis of GaN thin film 59

5.2.1 Pt/GaN hydrogen gas sensor 64

5.3 Analysis of $Al_{0.3}Ga_{0.7}N$ thin film 75

5.3.1 Pt/$Al_{0.3}Ga_{0.7}N$ hydrogen gas sensor 80

5.4 Analysis of $In_{0.3}Ga_{0.7}N$ thin film 88
5.4.1 Pt/$In_{0.3}Ga_{0.7}N$ hydrogen gas sensor 94
5.5 Analysis of $In_{0.5}Ga_{0.5}N$ QDs thin film 101
5.5.1 Pt/$In_{0.5}Ga_{0.5}N$ QDs hydrogen gas sensor 106
5.6 Summary 115

CHAPTER 6: CONCLUSION **117**
CHAPTER 7: FUTURE WORK **119**
REFERENCES
APPENDIX
PUBLICATIONS

LIST OF TABLES

		Page
Table 1.1	Some properties of wurtzite III-nitrides.	1
Table 1.2	Summary of hydrogen sources and production processes.	2
Table 1.3	The safety characteristics of combustibles.	3
Table 2.1	Industrial uses of hydrogen.	13
Table 2.2	Valence band offset and bowing parameters of the ternary alloys.	20
Table 4.1	Outgassing processes of Si (111) substrate prior the epitaxial layer growth.	48
Table 4.2	Growth details of AlN buffer layer.	50
Table 4.3	Growth details of GaN thin films.	52
Table 4.4	Growth details of AlGaN thin films.	52
Table 4.5	Growth details of InGaN thin films.	53
Table 4.6	Growth details of InGaN QDs thin films.	54
Table 4.7	The summary of growth conditions for III-nitrides thin films.	58
Table 5.1	The 2θ HRXRD peak positions of different crystal planes and their relative intensities.	63
Table 5.2	The summary of Pt/GaN hydrogen sensor characteristics at 0.1% H_2.	71
Table 5.3	Comparison of other GaN based hydrogen sensors.	73
Table 5.4	Sensitivity, response/recovery time and saturation current of the Pt/ GaN gas sensors for different concentrations of hydrogen ambience.	75
Table 5.5	The 2θ HRXRD peak positions of different crystal planes and their relative intensities.	78
Table 5.6	The summary of Pt/$Al_{0.3}Ga_{0.7}N$ hydrogen sensor characteristics at 0.1% H_2.	81
Table 5.7	Comparison of other AlGaN based hydrogen sensors.	87

Table 5.8	Sensitivity, response/recovery time and saturation current of the Pt/$Al_{0.3}Ga_{0.7}N$ gas sensors for different concentrations of hydrogen ambience.	88
Table 5.9	The 2θ HRXRD peak positions of different crystal planes and their relative intensities.	92
Table 5.10	The summary of Pt/$In_{0.3}Ga_{0.7}N$ hydrogen sensor characteristics at 0.1% H_2.	98
Table 5.11	Sensitivity, response/recovery time and saturation current of the Pt/$In_{0.3}Ga_{0.7}N$ gas sensors for different concentrations of hydrogen ambience.	100
Table 5.12	The comparison of different types of self-assembled InGaN QDs grown by MBE.	104
Table 5.13	The 2θ HRXRD peak positions of different crystal planes and their relative intensities.	105
Table 5.14	The summary of Pt/$In_{0.5}Ga_{0.5}N$ QDs hydrogen sensor characteristics at 0.1% H_2.	109
Table 5.15	Sensitivity, response/recovery time and saturation current of the Pt/$In_{0.5}Ga_{0.5}N$ QDs gas sensors for different concentrations of hydrogen ambience.	114
Table 5.16	Summary of III-nitrides-based hydrogen sensors with operating temperature of 400ºC.	116

LIST OF FIGURES

		Page
Figure 2.1	Schematic of a hydrogen fuel cell.	12
Figure 2.2	Schematic of electrochemical sensor.	14
Figure 2.3	The experimental set-up of PQCMB sensor.	15
Figure 2.4	Schottky diode sensor. (a) H2 dissociates on metal contact with catalytic metal. b) H atoms diffuse and form a dipole layer by OH bond that changes the I-V characteristics.	17
Figure 2.5	Bandgap values versus lattice constant of wurtzite III-nitrides and their respective ternary alloys.	18
Figure 2.6	Density of electron states of a semiconductor as a function of dimension. The optical absorption spectrum is roughly proportional to the density of states.	25
Figure 2.7	The splitting of energy level in QDS due to quantum confinement effect. The band gap of semiconductor increases with decrease in size of QDs.	26
Figure 3.1	Schematic view of a growth chamber in MBE system.	31
Figure 3.2	Basic operation of RGA.	33
Figure 3.3	Schematic diagram of the RHEED technique in an MBE system.	34
Figure 3.4	The sketch of the intensity of specular RHEED beam as a function of time.	35
Figure 3.5	The schematic view of FESEM.	36
Figure 3.6	Principle scheme of the atomic force microscopy.	38
Figure 3.7	Diffraction of X-rays by a crystal.	41
Figure 3.8	Typical experimental set-up for PL measurements.	43
Figure 4.1	UNI-block substrate holders on a trolley.	46
Figure 4.2	RGA measurement for leak detection.	47

Figure 4.3	RHEED pattern during the Ga cleaning process (a) before (b) after.	48
Figure 4.4	RHEED of Si surface during the Al flush.	50
Figure 4.5	RHEED pattern of AlN buffer layer (a) with Al high flux (b) normal Al flux.	51
Figure 4.6	The schematic of the InGaN QDs based hydrogen gas sensor.	55
Figure 4.7	Gas sensor set-up.	56
Figure 5.1	RHEED pattern of (a) AlN buffer layer (b) GaN epilayer.	60
Figure 5.2	(a) FESEM (b) EDX analyses of GaN thin film.	61
Figure 5.3	AFM images of GaN thin film.	62
Figure 5.4	HRXRD pattern of GaN thin film on Si (111).	63
Figure 5.5	PL spectrum of GaN thin film grown on Si (111) with the AlN buffer layer.	64
Figure 5.6	Typical I-V characteristics of Pt/GaN hydrogen sensor at different operating temperatures with 0.1% H_2 concentration.	65
Figure 5.7	The difference of Schottky barrier heights ($\Delta\Phi_B$) of Pt/GaN Schottky diodes 0.1% H_2 as a function of temperature.	68
Figure 5.8	Sensitivity of Pt/GaN gas sensor at different temperature.	70
Figure 5.9	Arrhenius plot of rate of current change of Pt/GaN gas sensor after exposure to 0.1% H_2 in N_2.	72
Figure 5.10	Sensitivity of Pt/GaN gas sensor at different hydrogen concentrations.	74
Figure 5.11	The response of Pt/GaN gas sensor at different hydrogen concentrations at optimum temperature of 400°C.	74
Figure 5.12	RHEED pattern of (a) GaN buffer layer (b) AlGaN epilayer.	76
Figure 5.13	(a) FESEM (b) EDX analyses of AlGaN thin film.	77
Figure 5.14	AFM of AlGaN thin film	77
Figure 5.15	HRXRD spectra of $Al_{0.3}Ga_{0.7}N$ on Si (111).	78

Figure 5.16 PL spectrum of $Al_{0.3}Ga_{0.7}N$ thin film grown on Si (111) with the AlN and GaN buffer layer. 80

Figure 5.17 Typical I-V characteristics of $Pt/Al_{0.3}Ga_{0.7}N$ hydrogen sensor at different operating temperature with 0.1% H_2 concentration. 82

Figure 5.18 The difference of Schottky barrier heights ($\Delta\Phi_B$) of $Pt/Al_{0.3}Ga_{0.7}N$ Schottky diodes 0.1% H_2 as a function of temperature. 83

Figure 5.19 Sensitivity of $Pt/Al_{0.3}Ga_{0.7}N$ gas sensor at different temperatures. 84

Figure 5.20 Arrhenius plot of rate of current change of $Pt/Al_{0.3}Ga_{0.7}N$ gas sensor after exposure to 0.1% H_2 in N_2. 85

Figure 5.21 Sensitivity of $Pt/Al_{0.3}Ga_{0.7}N$ gas sensor at different hydrogen concentrations. 87

Figure 5.22 RHEED pattern of (a) GaN (b) InGaN epilayer. 89

Figure 5.23 (a) FESEM (b) EDX analyses of InGaN thin film. 90

Figure 5.24 AFM images of InGaN thin film. 91

Figure 5.25 HRXRD pattern of InGaN thin film on Si (111). 91

Figure 5.26 PL spectrum of a $In_{0.3}Ga_{0.3}N$ thin film grown on Si (111) with the AlN and GaN buffer layer. 93

Figure 5.27 Typical I-V characteristics of $Pt/In_{0.3}Ga_{0.7}N$ hydrogen sensor at different operating temperature with 0.1% H_2 concentration. 95

Figure 5.28 The difference of Schottky barrier heights ($\Delta\Phi_B$) of $Pt/In_{0.3}Ga_{0.7}N$ Schottky diodes 0.1% H_2 as a function of temperature. 96

Figure 5.29 Sensitivity of $Pt/In_{0.3}Ga_{0.7}N$ gas sensor at different temperatures. 97

Figure 5.30 Arrhenius plot of rate of current change of $Pt/In_{0.3}Ga_{0.7}N$ gas sensor after exposure to 0.1% H_2 in N_2. 99

Figure 5.31 Sensitivity of $Pt/In_{0.3}Ga_{0.7}N$ gas sensor at different hydrogen concentrations. 100

Figure 5.32 RHEED pattern of (a) GaN wetting layer (b) InGaN epilayer (c) InGaN QDs. 101

Figure 5.33 (a) FESEM (b) EDX analyses of InGaN QDs thin film. 103

Figure 5.34 AFM images of InGaN QDs thin film. 103

Figure 5.35 HRXRD pattern of InGaN QDs thin film on Si (111). 105

Figure 5.36 PL spectrum of a $In_{0.5}Ga_{0.5}N$ QDs thin film grown on Si (111) with the GaN wetting layer. 106

Figure 5.37 Typical I-V characteristics of $Pt/In_{0.5}Ga_{0.5}N$ hydrogen sensor at different operating temperature with 0.1% H_2 concentration. 108

Figure 5.38 The difference of Schottky barrier heights ($\Delta\Phi_B$) of $Pt/In_{0.5}Ga_{0.5}N$ Schottky diodes 0.1% H_2 as a function of temperature. 110

Figure 5.39 Sensitivity of $Pt/In_{0.5}Ga_{0.5}N$ QD gas sensor at different temperatures. 111

Figure 5.40 Arrhenius plot of rate of current change of $Pt/In_{0.5}Ga_{0.5}N$ QD gas sensor after exposure to 0.1% H_2 in N_2. 112

Figure 5.41 Sensitivity of $Pt/In_{0.5}Ga_{0.5}N$ QDs gas sensor at different hydrogen concentrations. 114

Figure 5.42 The comparison of the sensitivity of III-nitrides based hydrogen sensor at different hydrogen concentrations. 115

LIST OF SYMBOLS

T	Absolute temperature
E_a	Activation energy
A	Area
θ_i	Coverage of hydrogen atoms
I	Current
ε	Dielectric constant
d	Distance
μ	Effective dipolemoment
m^*	Effective mass
m_o	Electron mass
E_g	Energy band gap
J_{Ga}	Ga flux
R	Gas constant
η	Ideality factor
θ	Incident / Diffraction angle
c	Lattice constant c
x	Mole fraction
J_N	N flux
N_i	Number of sites per area at the interface
k	Rate of current changes
A*	Richardson's constant
I_o	Saturation current
Φ_B	Schottky barrier height
$\Delta\Phi_B$	Schottky barrier height modulation

S	Sensitivity
V	Voltage
λ	Wavelength

LIST OF MAJOR ABBREVIATIONS

AFM	Atomic Force Microscopy
CAR	Continuous Azimuthal Rotation
I-V	Current-Voltage
DC	Direct Current
EDX	Energy Dispersive X-ray Spectroscopy
FESEM	Field Scanning Electron Microscopy
FM	Frank-van Der Merve
HRXRD	High Resolution X-ray Diffraction
IR	Infrared
LED	Light Emitting Diode
MFC	Mass Flow Controller
MS	Metal Semiconductor
MBE	Molecular Beam Epitaxy
ML	Monolayer
MQW	Multi Quantum Well
PL	Photoluminscence
PQCMB	Piezoelectric Quartz Crystal Microbalance
PAMBE	Plasma-Assisted Molecular Beam Epitaxy
PBN	Pyrolytic Boron Nitride
QD	Quantum Dot
RF	Radio Frequency
RF-MBE	Radio Frequency Plasma Assisted Molecular Beam Epitaxy
RHEED	Reflection High Energy Electron Diffraction
RGA	Residual Gas Analysis

RT	Room Temperature
SEM	Scanning Electron Microscope
SBH	Schottky Barrier Height
SAW	Surface Acoustic Wave
3D	Three Dimensional
2D	Two Dimensional
2DEG	Two-Dimensional Electron Gas
UHV	Ultra High Vacuum
UV	Ultra Violet
XRD	X-ray Diffraction
YL	Yellow Luminescence

HETEROSTRUKTUR III-NITRIDA YANG DITUMBUHKAN DENGAN RF-MBE UNTUK APLIKASI PENDERIAAN GAS HIDROGEN

ABSTRAK

Dalam teknologi hijau semasa, hidrogen (H_2) mempunyai potensi untuk bertindak sebagai pembawa tenaga yang baru dan sumber bahan api alternatif yang cekap dan mesra alam. Walau bagaimanapun, H_2 terkenal mempunyai sifat letupan dan mudah terbakar. Oleh itu, pembangunan penderia gas H_2 yang berprestasi tinggi untuk pemantauan dan pengesanan kebocoran dalam persekitaran yang sukar amat diperlukan untuk mengelakkan sebarang kemalangan maut. Jurang jalur lebar III-nitrida mempunyai keupayaan operasi kuasa/suhu yang tinggi dan juga rintangan kimia yang besar, oleh itu mereka boleh menjadi pilihan alternatif untuk aplikasi penderia gas pada suhu tinggi yang boleh beroperasi dalam persekitaran yang sukar. Dalam kerja ini, filem nipis III-nitrida (GaN, AlGaN, InGaN) dan dot kuantum (QDs) InGaN yang berkualiti tinggi telah ditumbuhkan di atas Si (111) dengan menggunakan epitaksi alur molekul berbantukan plasma (RF-MBE). Sifat-sifat struktur dan optik bahan-bahan telah dicirikan dengan pelbagai teknik pencirian. Bagi mendapatkan penderia gas pada suhu tinggi dengan kepekaan tinggi, peranti telah difabrikasikan dengan Pt sebagai sentuhan Schottky. Kepekaan penderia untuk pengesanan gas hidrogen telah dikaji pada suhu 100°C hingga suhu 500°C dengan kepekatan gas hidrogen yang berbeza. Dalam ukuran arus-voltan (I-V), penderia gas berasaskan III-nitrida menujukkan ciri rektifikasi. Penyerapan hidrogen ke peranti penderia memberi kesan penurunan sawar Schottky dan menyebabkan anjakan voltan. Kepekaan peranti meningkat dengan kenaikan suhu operasi disebabkan keaktifan penceraian H_2 ke atas logam pemangkin pada suhu yang lebih tinggi. Walau bagaimanapun, oksigen dalam fasa gas akan diserap pada permukaan peranti dan

bertindak balas dengan H_2 untuk menghasilkan air di permukaan Pt pada suhu lebih tinggi yang akan menyebabkan penurunan kepekaan penderia. Suhu operasi optimum untuk penderia gas berasaskan III-nitrida didapati pada suhu 400°C. Di samping itu, pengaruh kepekatan hidrogen terhadap prestasi penderia gas juga dikaji. Keputusan menunjukkan bahawa kepekaan dan masa bertindak balas peranti sentiasa meningkat apabila ambien hidrogen ditukar daripada 0.1% ke 2.0% yang menunjukkan bahawa peranti dapat mengesan perubahan kepekatan hidrogen pada suhu tinggi. Dalam perbandingan di antara semua sampel, Pt/InGaN QDs didapati mempunyai sensitiviti dan masa bertindak balas yang lebih baik iaitu 5.09 dan 320s masing-masing pada 2.0% hidrogen dengan suhu operasi 400°C. Selain itu, nilai tenaga pengaktifan (3.91 kcal/mol) yang kecil menunjukkan bahawa Pt/$In_{0.5}Ga_{0.5}N$ QDs mempunyai kepekaan yang lebih tinggi berbanding dengan peranti lain kerana nisbah kawasan permukaan dengan isipadu yang tinggi. Ianya didapati bahawa kawasan permukaan yang lebih besar pada $In_{0.5}Ga_{0.5}N$ QDs akan meningkatan kadar pemisahan molekul hidrogen dan pembentukan hidrogen atom. Keputusan menunjukkan bahawa penderia gas berasaskan III-nitrida mempunyai harapan untuk pengesanan hidrogen pada suhu yang tinggi. Sifat hidrogen penderiaan yang cemerlang bagi QDs boleh dibangunkan sebagai peranti penderia generasi akan datang.

RF-MBE GROWN III-NITRIDES HETEROSTRUCTURES FOR HYDROGEN GAS SENSING APPLICATIONS

ABSTRACT

In the current green technology, hydrogen (H_2) has the potential to act as new energy carrier and alternative fuel source that is efficient and eco-friendly. However, H_2 is well known to have excellent explosive and combustible properties. Hence, there is an absolutely necessity to develop high performance H_2 sensors for monitoring and leak detection in harsh environments to prevent any fatal accidents. The wide band gap III-nitrides have high power/high temperature operation capability and great chemical resistance, therefore they become an alternative option for high temperature gas sensor application which can operate in harsh environment. In this work, high quality III-nitrides thin films (GaN, AlGaN, InGaN) and InGaN quantum dots (QDs) were grown on Si (111) by using RF plasma assisted molecular beam epitaxy (RF-MBE). The structural and optical properties of materials were characterized by various characterization techniques. In order to achieve a high sensitivity, and high temperature hydrogen gas sensor devices, the devices were fabricated using Pt as Schottky contacts. The sensitivity of the sensors to hydrogen detection was studied at temperatures from 100^oC to 500^oC with different hydrogen concentrations. In the current- voltage (I-V) measurements, the III-nitrides based gas sensor showed rectifying properties. The adsorption of hydrogen onto the sensor devices results in an effective decrease of the Schottky barrier height, manifesting as a voltage shift. As operation temperature increases, the sensitivity of devices is increased due to the more active dissociation of H_2 on the catalytic metal at higher temperatures. However, oxygen in the gas phase will absorb on the device surface and react with H_2 to form water on the Pt surface at further higher temperature

resulted in decrease of the sensitivity sensor. The optimum operating temperature for III-nitrides based gas sensor was found at 400°C. In addition, the influence of hydrogen concentration to sensor performance was studied. The results show that the sensitivity and response time of devices was constantly increased when the hydrogen ambient is changed from 0.1% to 2.0% which indicated that the devices were able to detect changes of hydrogen concentration at elevated temperature. In the comparison of all samples, the Pt/InGaN QDs exhibits better sensitivity and response time which is 5.09 and 320s respectively at 2.0% hydrogen with the operating temperature of 400°C. Besides that, the small value of activation energy (3.91 kcal/mol) shows that Pt/$In_{0.5}Ga_{0.5}N$ QDs has higher sensitivity compared to other devices due to the high surface area to volume ratio. It is found that the larger surface area of $In_{0.5}Ga_{0.5}N$ QDs will allow more hydrogen molecules to dissociate and form atomic hydrogen efficiently. The results indicated that III-nitrides based gas sensors appear promising for hydrogen detection at high temperature. The excellent hydrogen sensing properties of QDs can be developed as next generation sensor devices.

CHAPTER 1
INTRODUCTION

1.1 Introduction to III-nitrides

GaN and its alloy compounds with AlN and InN form a direct wide band gap semiconductor family of great promise for optoelectronic and high power/high temperature application. GaN is a very attractive material for devices due to its wide band gap, high thermal and chemical stability. These characteristics allow the material to be used at elevated temperatures and in caustic environments where the properties of other semiconductor systems would degrade. The band gaps of III-nitrides span from infrared to ultraviolet (UV) spectra; 0.7 eV, 3.4 eV and 6.2 eV for InN, GaN and AlN respectively (Wu, *et al* 2002, Saito, *et al* 2002). Due to their wide band gap, III-nitrides are suited to use for blue and UV light emitting devices, high-density optical storage and full color display. Some properties of wurtzite III-nitrides from previous studies are shown in Table 1.1.

Table 1.1 Some properties of wurtzite III-nitrides ($_a$Wu, *et al* 2009, $_b$Hiroshi, 2002, $_c$Porowski, *et al* 1997, $_d$Mousam, *et al* 2012, $_e$Hovel, *et al* 1972).

Parameter	GaN	AlN	InN
$_a$Bandgap, E_g (T=300K) (eV)	3.43	6.14	0.64
$_a$Lattice Constant, a (T=300K) (Å)	3.189	3.112	3.533
$_a$Lattice Constant, c (T=300K) (Å)	5.185	4.982	5.693
$_b$Electron Effect Mass, m_o	0.20	0.48	0.11
$_b$Thermal Conductivity, κ (W/cmK)	1.3	2.0	0.8
$_b$Dielectric Constant, ε	8.9-9.5	8.5	15.3
$_b$Saturated Electron Drift Velocity, v_{sat} (10^7 cm/s)	2.5	1.4	2.5
Electrical Resistivity (T=300K) (Ω.cm)	$_c10^{-1}$	$_d{>}10^{14}$	$_e3\text{-}5\times10^{-3}$

Besides that, they also can stand at elevated temperatures and hostile environment. As a consequence of their large band gaps, GaN and AlN have high breakdown fields and low intrinsic carrier concentration (Hai, *et al* 2006). They also have high theoretical electron drift velocity and saturation current density. With these advantages, III-nitrides are among the most promising materials to extend the capabilities of optoelectronic devices.

1.2 Introduction to Hydrogen

Hydrogen is the simplest and lightest element on earth. An atom of hydrogen has only one electron and one proton. Hydrogen exists as gas at standard temperature and pressure. Hydrogen is an energy carrier but not an energy source, meaning that it can store and deliver energy in an easily usable form. Hydrogen can be produced from variety of sources which are listed in Table 1.2.

Table 1.2 Summary of hydrogen sources and production processes (Trygve, *et al* 2006).

Hydrogen sources	Production Processes
Coal	Gasification of coal
Oil	Steam reforming or partial oxidation of fossil oils
Gas	By-product from reforming natural gas or biogas with steam
Power	Water electrolysis by using any power source including wind, solar power and nuclear
Wood/Biomass	Decomposing biomass under controlled conditions
Algae	Photosynthesis
Alcohols	Biomass derived alcohols such as methanol and ethanol

Hydrogen gas is not freely available in the atmosphere but usually exists as a hydrogen containing compound mainly such as water (H_2O) and in the form of

hydrocarbons or fossil fuels. Besides that, hydrogen also can found in biomass, which includes all plants and animals.

1.3 Need of Hydrogen Sensor

Hydrogen monitoring in nitrogen atmospheres can be useful for atmosphere control in semiconductor industries. In metal industries, hydrogen sensor is used to quantify the hydrogen content to prevent the porosity in molten steel. Hydrogen sensor is also used in biological process to monitor the growth of anaerobic bacteria (Rasha, *et al* 2011). Table 1.3 shows basic safety relevant characteristics of hydrogen and other combustibles.

Table 1.3 The safety characteristics of combustibles (Hord, *et al* 1978, Eichert, *et al* 1986).

Properties	Hydrogen	Methane	Propane	Gasoline
Limits of flammability in air (vol %)	4.0-75.0	5.0-15.0	2.1-9.5	1.0-7.6
Auto-ignition temperature (°C)	585	540	487	228-471
Minimum energy for ignition in air (μJ)	20	290	260	240
Diffusion coefficient in air (cm^2s^{-1})	0.61	0.16	0.12	0.05
Flame Temperature (°C)	2111	1954	2112	2200
Limits of detonability in air (vol-%)	18.3-59.0	6.3-14.0	-	1.1-3.3
Detonation velocity in air (ms^{-1})	2000	1800	1850	1400-1700
Flame propagation velocity (ms^{-1})	3.46	0.43	0.47	-

Hydrogen is less dangerous compared to other combustibles due to high auto ignition temperature (585°C) but hydrogen is an invisible, odorless, and tasteless flammable gas which cannot be detected by human sense. It is highly flammable due to high heat of combustion and low ignition temperature with the wide flammable range of 4%-75%. The smallest hydrogen molecule has a high diffusion

coefficient in air which makes leakage a problem at all stages of usage such as storage and fuel cell in transportation.

Thus, it is necessary to develop a safety monitoring system for detecting the hydrogen level using affordable and compact hydrogen sensors to prevent the risk of a fatal accident due to hydrogen leakage as they can signify potentially hazardous conditions. Besides that, hydrogen will cause corrosion at elevated temperature (Robert, 1996). The hydrogen atoms penetrate into the metals and subsequently exasperate the metals internally, which will affect the properties of metals such as strength, durability and fracture toughness. Hence, the need to develop a hydrogen sensor with high sensitivity and fast response at high temperature has gained momentum with the advent of hydrogen sensor technology.

1.4 Hydrogen sensor parameters

The five basic parameters of the entire gas sensor are the sensitivity, selectivity, response time, recovery time and stability. These parameters are the key characteristics of the gas sensor performance. The sensitivity is basic measureable parameters for a gas sensor characteristic. It is a variation in chemical/physical properties of sensing material under target gas exposure. The sensitivity of a Schottky diode gas sensor can defined as the ratio of the change in the current of the thick film upon exposure to the target gas. The equation is given below:

$$Sensitivity = \frac{I_{gas} - I_{Air}}{I_{Air}} \tag{1.1}$$

where I_{Air} and I_{gasA} are currents measured in air and target gas containing ambience, respectively.

Selectivity is the ability of a gas sensor to respond to single analyte gas without being affected by the presence of other interference gases under same condition. The selectivity of a gas sensor can be defined as the ratio of the sensitivity of single target analytes gas relative to another analyte gas.

$$Selectivity = \frac{Sensitivity_{gasA} - Sensitivity_{gas}}{Sensitivity_{gasA}} \qquad (1.2)$$

Response time is typically defined as the time required for the gas sensor to reach 90% (T_{90}) of full scale after being exposed to the target gas. The time for the output of a gas sensor to return to its initial value after the removal of the target gas is defined as recovery time. For the commercial gas sensor, the recovery time was usually specified as time to fall to 10% of steady state value after the removal of the measured gas. The commercial usage of gas sensor is highly dependent on the response time and recovery time. The small value of response time and recovery time indicated better application in the market compared with the one with long recovery and response time. Stability is the ability of a sensor to maintain or repeatability of its performance characteristics for a given period of time.

1.5 III-nitrides based hydrogen sensor

There are many different Schottky diode metal semiconductors (MS) hydrogen sensors that were studied in the past decades (Lechuga, *et al* 1991, Chou, *et al* 2005,

Luther, *et al* 1999). These sensors use catalytic metals such as palladium (Pd) and platinum (Pt) as sensing metals due to easily dissociate hydrogen molecules. In the MS hydrogen sensor, a dipole layer was created after the hydrogen atoms diffuse into the MS interface. This layer will lower the effective work function of the catalytic metal and change the electrical properties of the devices.

Among the wide band gap semiconductors, GaN based semiconductor materials are the most promising for gas sensor devices that operate in harsh environmental conditions such as high-temperature and chemically corrosive ambient due to their good thermal and chemical stability. In addition the small Fermi level pinning characteristics of III-nitrides are also important features that may lead to high gas sensor sensitivity (Zhao, *et al* 2003). Besides that, III-nitrides MS sensors are more economical compared to other materials due to simple processing steps. For these reasons, III-nitride semiconductor materials have attracted much attention in the field of gas sensing application.

In addition, III-nitrides nanostructured based gas sensor can reduce the working temperatures and they consume less power operation as well as safer operation (Jimenez, *et al* 2007). One dimensional (1D) nanostructures, such as nanowires, nanorods and nanobelts, are particularly suited for chemical sensing due to their large surface to volume ratio (Comini, *et al* 2010, Sharadrao, *et al* 2015, Carlos, *et al* 2015). The high area/volume ratio will also improve the adsorption of gases on the surface sensor and increase the sensitivity of the devices.

1.6 Motivations

As mention above, hydrogen gas has high diffusion coefficient in air and easily leak due to small and light molecules. Therefore, the development of technologies for monitoring and detection application will be of vital importance for life safety to prevent any accident due to hydrogen leakage. The sensor must have high sensitivity, selectivity, repeatability and rapid response times. For the development of reliable and efficient hydrogen sensors for process monitoring and leak detection applications, *in situ* monitoring of processes are used and require the sensors to be operated in harsh environments. Harsh environment can be referred to situations involving high power, high temperature, high aggressive media exposure, and high radiation. Significant corrosion related degradation will be caused by harsh environment. To date, typically numerous harsh environment applications are related to automobiles, nuclear power plant, and aerospace as well as communications industries.

In order to make the sensor function in these environment, a cooling system is required to maintain the stable operation. This will increase the operation cost and limit the space of the system to integrate other electronics components. As a result, the efficiency and reliability of the system will become lower. Hence, sensing structures and materials capable of withstanding such conditions are being exhaustively investigated. Therefore, the main purpose of this work is to study and develop a simple, low cost and high sensitivity III-nitrides based hydrogen gas sensor which can operate at different high temperature up to 500°C with different ambient

gas concentrations. Fabrication of III-nitrides based hydrogen sensor on Si substrates is more economical than many other sensors due to inexpensive materials and a reduced number of processing steps.

1.7 Objectives

The objectives of this work are:

1. To study the growth of III-nitrides (GaN, AlGaN, InGaN) thin films and InGaN QDs on Si (111) by using RF plasma-assisted molecular beam epitaxy (RF-MBE).
2. To investigate the structural and optical properties of III-nitrides thin films.
3. To study the sensing performances (sensitivity, response and recovery time) of III-nitrides based metal semiconductor (MS) hydrogen sensor.
4. To explore the feasibility of III-nitrides for hydrogen sensor applications over the wide range of high operating temperatures and gas concentrations.

1.8 Originality of the research works

In this work, high quality InGaN QDs was successfully grown on Si (111) by RF-MBE without growth interruption at reduced temperature (500°C-600°C). From the literature, the growths of self-assembled InGaN QDs on Si (111) by RF-MBE are relatively less investigated as compared to sapphire especially at low temperature growth. In addition, the high temperature III-nitrides based hydrogen sensors were successfully fabricated. Although many III-nitrides based hydrogen sensor were

proposed by many researchers, there were no reports for III-nitrides based hydrogen sensor on Si (111) that can operate at elevated temperatures (>250°C).

The fabrication of high sensitive III-nitrides nanostructured hydrogen gas sensors for elevated temperature detection is a key to the development of novel hydrogen-based technologies. To date, there are various nanostructures such as GaN nanowires (Abdullah, *et al* 2015, Wright, *et al* 2009) and ZnO nanowires (Aurel, *et al* 2015, Niranjan, *et al* 2013) which are synthesized for gas sensing applications with excellent response and recovery characteristics. However, there were no report on H_2 gas sensors based on III-nitrides QDs, which may offer excellent environmental stability as well as enhanced sensitivity and speed of response of the sensors. Additionally, many gas detecting sensors are not able to maintain sensitivity and stability at high temperatures due to chemical reactions occurring between the catalytic metal sensing layer and substrate layer. High temperature gas sensors based III-nitrides on Si (111) are relatively new and unstudied. The advanced study will lead wider commercial applications for high temperature hydrogen sensors in near future.

1.9 Organization of the thesis

The present work is divided into six chapters which present the complete picture of the work carried out. The second chapter includes the literature review relevant to this work. A brief theory and characteristics of hydrogen sensing as well as the fabrication techniques are included in this chapter.

The third chapter consists of the common knowledge and the theory of the equipment tool. The fourth chapter covers the experimental techniques used for the preparation and characterization of III-nitrides based hydrogen gas sensor. It begins with the growth details and characterization of the III-nitrides thin films and QDs followed by fabrication of hydrogen gas sensors by using Pt catalytic contacts. The fifth chapter presents results of the physical, electrical and gas sensing characterization of III-nitrides based hydrogen sensor. Various comparisons of results obtained using different experimental procedures such as different temperature and ambient gas concentration are presented here. Final chapter covers the conclusion of this project and provides some ideas for future work.

CHAPTER 2
LITERATURE REVIEW

2.1 Introduction

The fundamental knowledge concerning this project is introduced in this chapter. The purpose of this chapter is to understand the background information on hydrogen technologies to establish the importance of hydrogen detection. A detailed literature review has been reviewed before deciding on pursuing the proposed high temperature III-nitrides based hydrogen sensor technology.

2.2 Hydrogen technology

Recently, hydrogen has become one of the most promising clean energy sources relating to varied applications in transportation instead of petroleum. Hydrogen fuel cell is much greater than the engines using hydrocarbon fuels and become an environmentally friendly fuel because the combustion product of hydrogen is only heat and water which is free from contamination and can be reproduced for periodic duty. The hydrogen fuel cell has two electrodes where the reactions take place and an electrolyte which carries the charged particles from one electrode to the other which was shown in Fig. 2.1. The fuel cell needs hydrogen and oxygen to work out.

When the hydrogen enters the anode, a chemical reaction strips the hydrogen molecules of their electrons to form H^+ ions. The electrons travel through wires to provide a current. In the meantime, the oxygen from the air will enters at the

cathode and picks up the electrons from anode and generates the electricity. The water will formed when the oxygen combines with the ionized hydrogen atoms (H^+).

Some limited productions of hydrogen powered car are already existed. The Honda FCX Clarity uses a hydrogen fuel cell and an electric motor. The fuel cell produces electricity by converting hydrogen and oxygen from the air that can be used as a clean alternative to gasoline. The BMW Hydrogen 7 has the ability to run on both hydrogen and gasoline using an internal combustion engine. Toyota Mirai is the first hydrogen fuel cell vehicle to be sold commercially in 2014.

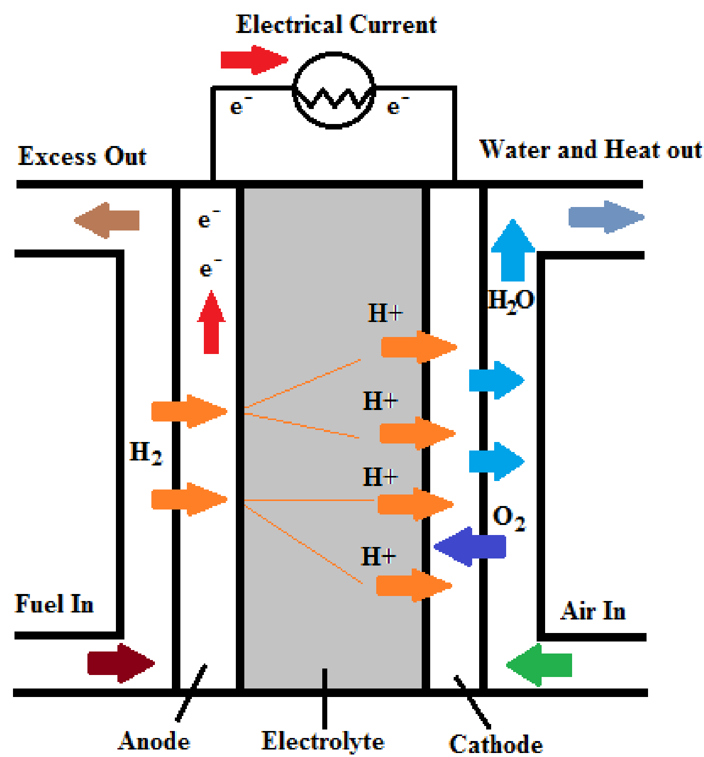

(a)

Fig. 2.1 Schematic of a hydrogen fuel cell.

In the food processing industry, hydrogen can be used in hydrogenation process to convert vegetable oils into solid or semi-solid fats which are necessary for the

manufacture of margarine. Hydrogen is also used primarily in the production of methanol and ammonia as well as for the purposes of the refining industry. Table 2.1 shows the use of hydrogen in different industries.

Table 2.1 Industrial uses of hydrogen (US Welding, 2003).

Industry	Application of hydrogen gas
Chemical processing	Primarily to manufacture methanol and ammonia, but also to hydrogenate non-edible oils for plastics, ointments, soaps, insulation and other specialty chemicals.
Metal production and welding	As a protective atmosphere in high temperature operations such as stainless steel manufacturing and hardening. Hydrogen can mix with argon for welding austenitic stainless steel and cutting operations as well as support plasma welding.
Pharmaceuticals	Used to produce vitamin C and A, surfactants, adhesives and sorbitol (sugar substitute) which is used in cosmetics.
Electronics	To create specially controlled atmospheres in the production of semiconductor circuits.
Petroleum Recovery and Refinery	To enhance performance of petroleum products by convert heavy crude to lighter, as well as to removing organic sulfur from crude oil.
Power Generation	React with O_2 for the cooling water system in nuclear reactor and high speed turbine generators.

2.3 Hydrogen gas sensor technology

Numerous types of hydrogen gas sensors based on different structures have been currently proposed, involving electrochemical sensor, piezoelectric, fiber optic, and Schottky diode. Most of the hydrogen sensor use catalytic metals such as platinum

(Pt) and palladium (Pd) due to a high hydrogen solubility and sensitivity for hydrogen molecules for this metal group. The absorption rate of hydrogen in these catalytic metals is dependent on hydrogen concentration and operating temperature.

Childs, *et al* (1978) developed the first electrochemical sensor. Electrochemical sensors are composed of an anode and cathode which is similar to fuel cell. The schematic of an electrochemical sensor is shown in Fig. 2.2. Electrochemical sensors operate by reacting with the gas of interest to produce an electrical signal proportional to that gas concentration. The disadvantage of this sensor is that it is not environmentally independent due to oxygen required for long term stability.

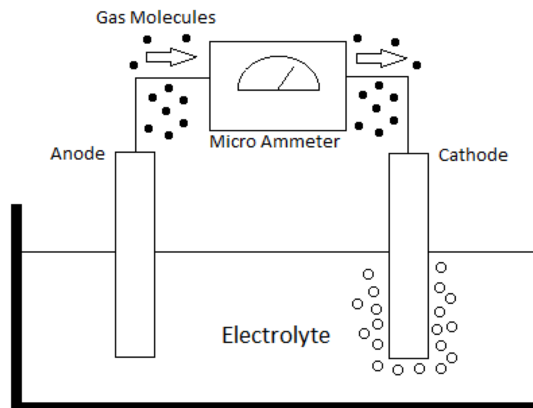

Fig. 2.2 Schematic of electrochemical sensor (Jack, 1999).

Piezoelectric field sensor can be divided into two categories which are piezoelectric quartz crystal microbalance (PQCMB) sensor and surface acoustic wave (SAW) sensor. PQCMB consists of an oscillator powered by a regulated power supply, ensuring that the applied voltage is constant. An experimental set up of the PQCMB is shown schematically in Fig. 2.3. The frequency meter was used

to measure frequency output from the oscillator. The response of the PCQMB sensor can be detected as a change in resonant frequency of the quartz crystal which depends on the mass of the chemically sensitive layer. The resonant frequency will decrease when the hydrogen molecules are absorbed in Pd layer, therefore the concentration of hydrogen can be measured with the change in the resonant frequency.

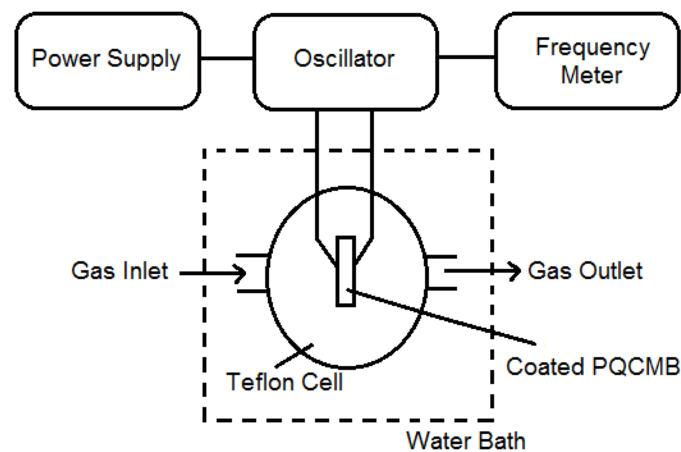

Fig. 2.3 The experimental set-up of PQCMB sensor (Christofides, 1990).

The first SAW sensor was discovered by D'Amico, *et al* (1982-1983). Sensing with acoustic wave is based on measuring variations of acoustic propagation velocity of wave, or wave attenuation. The SAW characteristics such as phase, velocity and amplitude will be changed when the hydrogen molecules are absorbed in a Pd or Pt layer. The SAW sensor has higher sensitivity compared to PQCMB due to higher resonant frequency.

Among the semiconductor sensors, Schottky diodes have been reported as widely

used devices in electronics and sensors industries because they are cheap and involve simpler fabrication procedures and electronic circuitry required for operation. Schottky diode is well known as metal semiconductor (MS) junction and also often recorgnized as a "surface barrier diode". Schottky contacts are formed when a metal of generally large work function is in contact with a semiconducting substrate. By employing an interfacial layer between the metal and the substrate, the Schottky diode can be utilized as a gas sensor.

The sensitivity of the Schottky diode based sensors is measured as a change in voltage or current, whilst the sensor is biased at a constant current or voltage, respectively. Many of them use catalytic metals such as palladium (Pd) or platinum (Pt) as a hydrogen trap because these metals have high hydrogen solubility and can selectively absorb hydrogen gas. The simple Schottky diode gas sensor is shown in Fig. 2.4.

When the gas sensor surface exposed to the hydrogen gas, the hydrogen molecules will catalytically dissociate through the metal to form a dipole layer which will lead to a modulation of the barrier height and the difference of I-V characteristics (Kim, *et al* 2003). The absorption of hydrogen in the catalytic metals depends on temperature and hydrogen concentration. Therefore, low power consumption, low cost, easy fabrication, high sensitivity and reliability are the main advantages of the Schotty diode semiconductor sensors.

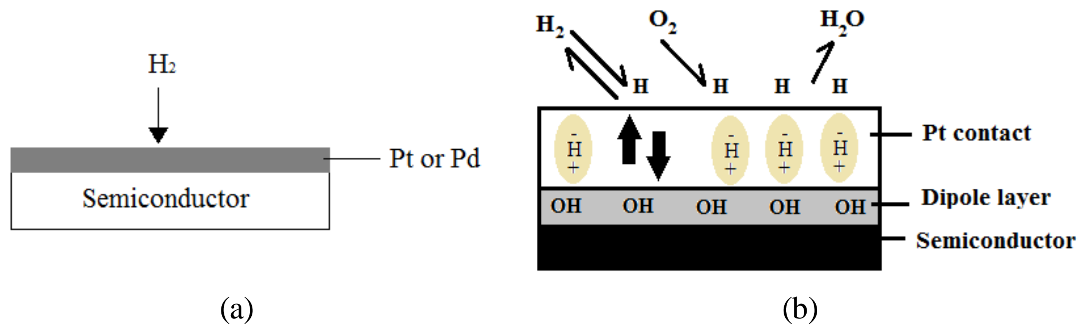

Fig. 2.4 Schottky diode sensor. (a) H_2 dissociates on metal contact with catalytic metal. b) H atoms diffuse and form a dipole layer by OH bond that changes the I-V characteristics (Ambacher, *et al* 2008).

2.4 III-Nitrides based gas sensor

The III-nitride materials have attracted an enormous amount of interest due to their wide direct band gap, outstanding electrical and mechanical properties, as well as potential applications in electronic (Mishra, *et al* 2007 and Xing, *et al* 2001), photovoltaic (Trybus, *et al* 2006, Trybus, *et al* 2008 and Wu, *et al* 2003), and light emitting devices (Nakamura, *et al* 1991, Nakamura, *et al* 1994, Nakamura, *et al* 1999 and Mukai, *et al* 2004). GaN with a bandgap of 3.4 eV was first synthesized by Parsons and Johnson in 1932 (Johnson, *et al* 1932) and it was the most popular binary nitride in III-nitrides group. The III-nitride material system has become particularly intriguing for use in optoelectronic applications right after the discovery of InN (Juza, *et al* 1938) and AlN (Ott, *et al* 1924) due to its tunable bandgap by forming alloys of the three binaries (Mohammad, *et al* 1996). The bandgap of InN has been revised to 0.7 eV (Davidov, *et al* 2002), which will expand the range of bandgaps achievable by the III-nitride materials to span the entire visible spectrum.

The band gaps and lattice spacing of the III-nitride and related alloys are shown in Fig. 2.5.

Gas sensing with high sensitivity and low detection limit in harsh environment is eagerly required in many applications such as chemical process monitoring and fuel cell. High temperature gas sensor materials need a high melting point and high thermal stability to withstand elevated temperature operation. Therefore, III-nitrides become candidates for high temperature gas sensing application due to their electrical and mechanical properties. The wide temperature stability and good chemical stability as well as mechanical robustness allow GaN based hydrogen sensor to be operated in harsh environment.

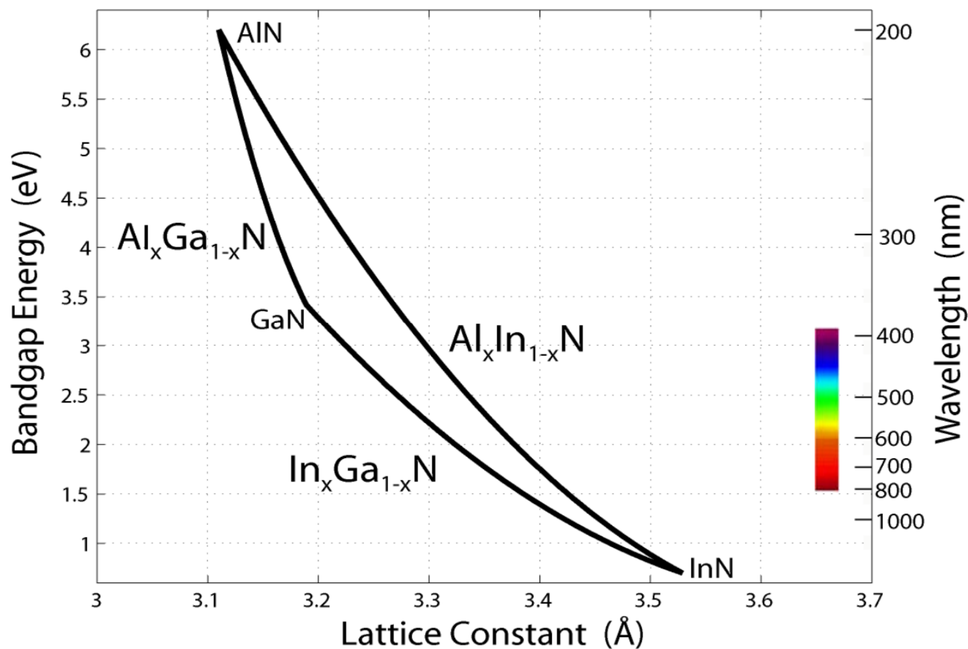

Fig. 2.5 Bandgap values versus lattice constant of wurtzite III-nitrides and their respective ternary alloys (Ibach, *et al* 2003).

Historically, there have been reports on GaN gas sensors utilizing Schottky contacts (Schalwig, *et al* 2002, Jihyan, *et al* 2003 and Weidemann, *et al* 2003), using

catalytic metals such as Pd or Pt. All the devices have detection ranges typically below the combustion point which is below 4.7% hydrogen. The first high temperature Pt/GaN/Al_2O_3 Schottky diode hydrogen sensor which can operate at the temperature range of 200°C-400°C was reported by Luther, *et al* (1999). Huang, *et al* (2007) and Wright, *et al* (2009) reported that their GaN/Si hydrogen sensor can operate at 100°C with the sensitivity of 0.18 and 0.04 respectively. However, to date, a high quality Pt/GaN/Si (111) hydrogen sensor that can operate at high temperatures (> 200°C) is studied less compared to GaN on SiC and sapphire substrates.

2.4.1 AlGaN based gas sensor

$Al_xGa_{1-x}N$ alloy is of interest as optoelectronic devices due to its tunable energy band gap (Strite, *et al* 1992). The direct energy band gap of this material lies in a typical range of 3.42 (for x = 0) to 6.1 eV (for x = 1) at 300K. The energy band gap of $Al_xGa_{1-x}N$ can be calculated approximately by

$$E_g(\text{AlGaN}) = xE_g(\text{AlN}) + (1-x)E_g(\text{GaN}) - bx(1-x) \tag{2.1}$$

where E_g(AlN) and E_g(GaN) are the band gaps of AlN and GaN respectively with the corresponding values of 0.7 eV and 3.4 eV, while the b is the bowing parameter with the value of 0.7 (Martin, *et al* 1996, Vurgaftman, *et al* 2003) for $Al_xGa_{1-x}N$ which is summarized in Table 2.2.

The Al mole fraction, *x* along with the $Al_xGa_{1-x}N$ barrier thickness are extremely important in determining the characteristics of AlGaN heterostructures. It influences the amount of polarization charges and two dimensional electron gas (2DEG) mobility as well as the depth of the quantum well where sheet charges are confined. A higher Al mole fraction results in a larger conduction band discontinuity and a higher bandgap which is beneficial in greater carrier confinement at the AlGaN/GaN interface that allow high mobility to coexist with a large carrier density (Wu, *et al* 1998). However, a high Al composition causes challenges in growing good quality and thick AlGaN layers since its lattice mismatch with GaN increases correspondingly. The large lattice mismatch (17%) (Wu, *et al* 2006) leads to surface cracking due to faster relaxation of the AlGaN layer (Thiele, *et al* 2005 and Wang, *et al* 2012).

Table 2.2 Valence band offset and bowing parameters of the ternary alloys (Martin, *et al* 1996, Vurgaftman, *et al* 2003).

Parameter	AlGaN	InGaN	InAlN
Valence band offset (eV)	-0.7	-1.1	-1.8
Alloy bandgap bowing (eV), *b*	0.7	1.4	2.5

Recently, interest in UV optoelectronics and gas sensor has led to focused research in the $Al_xGa_{1-x}N$ alloys, as it provides for a suitable material system for the realization of these applications. The intrinsic polarization fields on the AlGaN/GaN surface are accepted to play an important role in determining the gas sensitivity and responsibility. Matsuo, *et al* (2005) found that increase of reverse and forward currents was much larger in the Pt/AlGaN compared to Pt/GaN.